PHASE-LIFETIME SPECTROSCOPY OF PHOTOCYCLE PROCESSES

Kinetic Analysis of Amplitude Dispersion Curves

T. G. DEWEY
Department of Chemistry, University of Denver, Denver, Colorado 80208

ABSTRACT Phase-lifetime spectroscopy has been recently used to obtain kinetic information on biological photocycles. A simple, general method is presented for deriving the amplitude response function for light-driven processes. These amplitude response functions may be used to analyze the experimental data obtained when driving the photosystem with a mechanically chopped, actinic light source. This analysis allows a comparison of kinetic parameters obtained from modulation methods with those obtained by flash techniques. Typically the experimental data consist of the signal amplitude measured at several chopping frequencies of the actinic light. These amplitude dispersion curves will be dependent on the harmonic sensitivity of the phase-sensitive detector used to measure the signal. This harmonic sensitivity is taken into account by performing a Fourier decomposition on the amplitude response function of the system and weighting each harmonic in a fashion appropriate for the specific amplifier under consideration. The resulting response function obtained for two commonly used amplifiers is derived. In addition to simple photocycles, the analysis of photocycle-coupled processes is also considered. This second relaxation process, which is coupled to a photocycle process, could represent the chemiosmotic coupling of a light-driven ion pump to a second ion transport protein. Conditions are established in which the kinetics of the second process can be resolved from the photocycle process.

INTRODUCTION

In recent years there has been increased use of phase modulation techniques to study biochemical photocycle processes (1–7; Sinton, M., and T. G. Dewey, manuscript in preparation). In most applications the response of a physical property is monitored while the photosystem is driven by a modulated actinic light source. Traditionally modulation techniques have been used to measure spectral properties of intermediates (9), whereas flash techniques have been favored for kinetic measurements. However, precise kinetic information can be obtained with modulation methods. These methods offer an advantage over flash techniques in that much lower actinic light intensities can be used. This reduces problems with sample bleaching and provides experimental conditions much closer to the physiological ones. Kinetic parameters can be obtained in two ways using modulation excitation. First, the phase difference, ϕ, between the probe signal and the actinic signal, can be measured with phase-sensitive detection. The relaxation time, τ, for the observed process is then given by tan $\phi = \omega\tau$ where ω is the radial frequency of the modulation. The disadvantage of this approach is that the phase relationships become complicated once more than one process is present. A second method is to measure the signal amplitude as a function of modulation frequency. This amplitude dispersion can be analyzed (3, 4) to determine amplitudes and lifetimes for multiple relaxation processes. The precise analysis of this type of information depends on the specific quantity measured by the amplifier and by the harmonic sensitivity of the amplifier. In general, lifetimes measured with these modulation techniques have compared quite favorably with those determined by flash methods (7). However, it is possible to have conditions where the two techniques will give different results. The goal of this paper is to present a theoretical foundation for the interpretation of phase-lifetime results. This will provide a basis for comparison of these results to results obtained by flash methods.

The theoretical basis of a chemical relaxation response to a periodic perturbation has been well established (10). In most applications the system, which is at equilibrium, is assumed to respond linearly to a perturbation in one of the thermodynamic variables. The individual, chemical species present will respond to the change in their chemical potential caused by the periodic perturbation of the thermodynamic variable. A photocycle driven by a periodic actinic light source provides a similar but not identical situation. In this case the perturbation is driving the system through a single component, the ground state of the absorbing species. Since the ground state will not convert to a photocycle state during the "off" cycle of the actinic light, the relaxation of the system will not be identical during the "on" and "off" cycles. This phenomenon has in fact been observed experimentally by Krupinsky and Hammes (7). This behavior is in contrast to the traditional

example of chemical relaxation after perturbation of a thermodynamic variable. In this latter case the relaxation time will be the same regardless of the direction by which equilibrium is approached (cf. 11). Despite these differences, it is appropriate in most applications of phase-lifetime spectroscopy to use the amplitude response function derived for traditional chemical relaxation. The rationale for this is presented in this paper.

In this work a general method is developed for deriving the amplitude response function for light-driven processes. A detailed analysis of a simple photocycle is presented. A photocycle is considered in which a single ground state species is driven by a square wave, actinic light source to yield a single intermediate. In most experiments the actinic light is mechanically chopped and, therefore, represents a periodic, square wave, forcing function. The amplitude response function obtained for this specific photocycle has a general mathematical form that will appear in response functions to most simple photocycles. This will be demonstrated in an accompanying experimental paper in which more complicated cycles are used to analyze experimental data for proton uptake kinetics of bacteriorhodopsin (Sinton, M., and T. G. Dewey, manuscript in preparation). In addition to determining the amplitude response function for the chemical species involved in the photocycle, the modification of this response function by the harmonic sensitivity of the detector is also considered. To describe the experimentally observed response function a Fourier decomposition of the amplitude response function is performed. The Fourier components of this function are then weighted by the known harmonic sensitivity of the lock-in amplifier. The final section of the paper considers the situation where a process associated with the modulated photocycle is used to drive a second process. An experimental application of this situation would be to use the membrane potential generated by the light-driven proton pump, bacteriorhodopsin, to drive chemiosmotic-coupled reactions catalyzed by a second membrane-bound protein. Thus, the modulation of the actinic light is coupled to the second process by the proton pumping of the bacteriorhodopsin. In this case the periodic forcing function is no longer a square wave but the exponential rise and decay of the concentration of transported protons. The amplitude response function for the relaxation of the second chemiosmotic process is derived. Simulated amplitude dispersion curves are calculated to show the range of relaxation times that can be measured relative to the relaxation time of the photocycle.

AMPLITUDE RESPONSE FUNCTION FOR A SIMPLE PHOTOCYCLE

In this section the amplitude response function is derived for the following process:

$$A \underset{k_{-1}}{\overset{k_1}{\rightleftharpoons}} B, \tag{1}$$

where A is the ground state species and B is the photocycle intermediate. The rate constant, k_1, is assumed to be proportional to the light intensity, I, and is given by $k_1 = k_0 I$ where k_0 is the appropriate rate constant. The constant k_{-1} is the unimolecular rate constant for the decay of the photocycle intermediate. In deriving expressions for the photocycle response to the square wave perturbation of the actinic light (see Fig. 1), the rate expressions for the photocycle are considered separately for the "on" cycle ($0 < t < \pi/\omega$) and for the "off" cycle ($\pi/\omega < t < 2\pi/\omega$). These expressions are given by:

$$-d[A]/dt = k_1[A] - k_{-1}[B]$$
$$= (k_1 + k_{-1})[A] - k_{-1}[A]_o \quad 0 < t < \pi/\omega \tag{2}$$

$$-d[A]/dt = -k_{-1}[B] = k_{-1}([A] - [A]_o)$$
$$\pi/\omega < t < 2\pi/\omega, \tag{3}$$

where $[A]_o = [A] + [B]$. The solutions of Eqs. 2 and 3 are given by Eqs. 4 and 5, respectively.

$$[A(t)] = \frac{k_{-1}[A]_o}{(k_1 + k_{-1})} - \left[\frac{k_{-1}[A]_o}{(k_1 + k_{-1})} - A_{on}\right] e^{-t(k_1 + k_{-1})} \tag{4}$$

$$[A(t)] = A_{off} e^{-k_{-1}t}, \tag{5}$$

where A_{on} is the concentration of A at the beginning of the "on cycle," i.e., $t = 2n\pi/\omega$ where n is any positive integer, and A_{off} is the concentration at the beginning of the "off cycle," $t = [\pi(2n - 1)/\omega]$. As can be seen by these equations, both the "on" and "off" cycles follow exponential time courses. The relaxation time during the "on cycle" should be shorter than the relaxation time during the "off cycle." This behavior has been observed experimentally by Krupinsky and Hammes (5) for the photocycle of bacteriorhodopsin. Eqs. 4 and 5 are coupled by the requirement that the concentration of A must be continuous when proceeding from the "on cycle" to the "off cycle." Thus, using Eq. 4, $\{A[\pi(2n - 1)/\omega]\} = A_{off}$. With Eq. 5, $[A(\pi 2n/\omega)] = A_{on}$. At steady state it can be assumed that $[A(\pi n/\omega)] = [A(\pi(n + 2)/\omega)]$. These relationships allow the amplitude, $\Delta A = A_{on} - A_{off}$, to be calculated. This amplitude is given by Eq. 6:

$$A = \left[\frac{k_{-1}[A]_o}{k_1 + k_{-1}}\right] \frac{(1 - e^{-\pi/\omega\tau_1})(1 - e^{-\pi/\omega\tau_{-1}})}{(1 - e^{-\pi/\omega\tau_1} e^{-\pi/\omega\tau_{-1}})}$$
$$= \left[\frac{2k_{-1}[A]_o}{k_1 + k_{-1}}\right] \frac{\tanh(\pi/2\omega\tau_{-1})}{1 + \tanh(\pi/2\omega\tau_{-1}) \coth(\pi/2\omega\tau_1)}, \tag{6}$$

where $1/\tau_1 = k_1 + k_{-1}$ and $1/\tau_{-1} = k_{-1}$. When k_1 is small, than τ_1 is approximately equal to τ_{-1}. This condition exists at low light intensities. Under these conditions Eq. 6 reduces to the following simple expression:

$$A = 2[A]_o \tanh(\pi/2\omega\tau_{-1}). \tag{7}$$

Thus, it is beneficial to perform modulation excitation experiments at low light intensities so that the amplitude

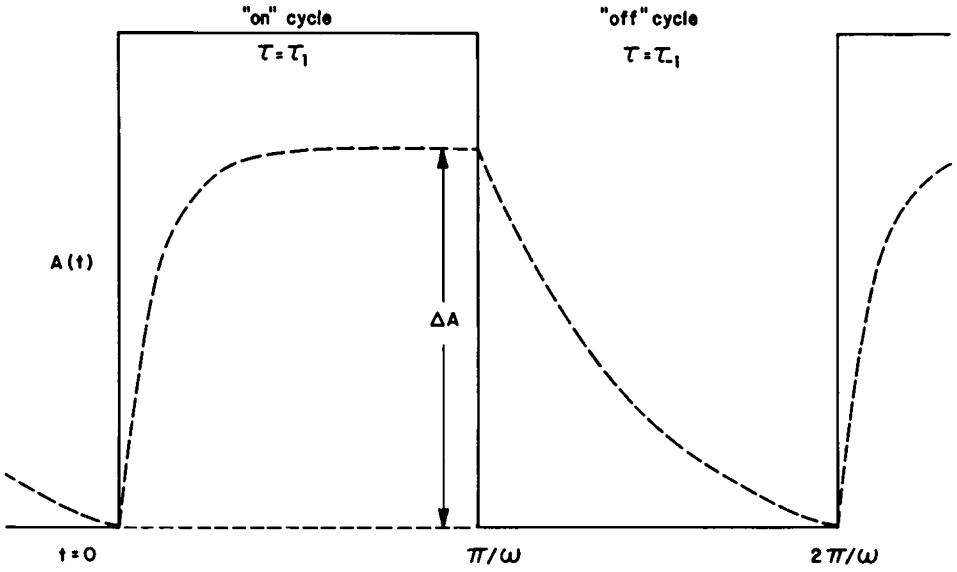

FIGURE 1 Time course of chopped actinic light intensity (*solid line*) and photocycle intermediate (*dashed line*) over a modulation cycle. The "on" cycle is defined for time, $t = 0$ to π/ω. The "off" cycle is from $t = \pi/\omega$ to $2\pi/\omega$. In this example, the relaxation times for the "on" and "off" cycles are different. The steady-state amplitude, ΔA, is given by Eq. 6.

response function will have a simpler form. Fig. 2 shows amplitude dispersion curves calculated from Eq. 6 for different values of the two relaxation times. As can be seen, the curves are sensitive to differences in these values. However, highly accurate data are required to distinguish a dispersion curve with two relaxation times from a curve in which the rise and decay times are the same. Thus, it may be difficult to accurately determine relaxation times in the former case. Under conditions of low light, phase-lifetime spectroscopy can be used to determine the rate of decay of the photocycle intermediate. This should be identical to the intermediate's decay rate constant observed in flash experiments. At higher light intensities it is in principle possible to obtain k_1. This would correspond to the rate constant for formation of the intermediate measured in a flash experiment. However, since this constant will be dependent upon the light intensity and the quantum yield, it will be very dependent upon the experimental conditions. If modulation experiments at high light intensities are analyzed as a single decay process, e.g., using Eq. 7, then an erroneous decay rate will be obtained.

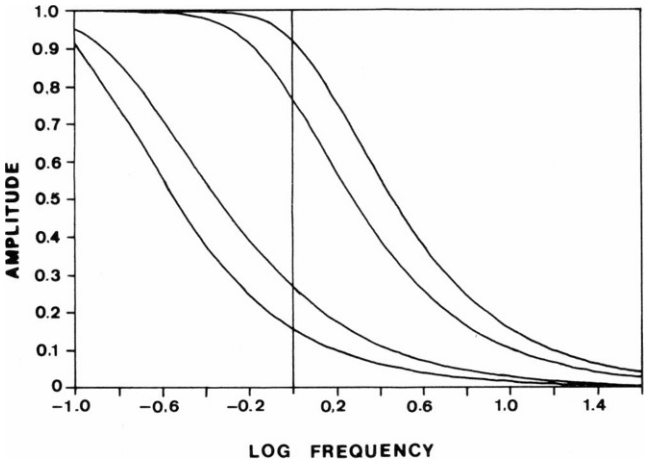

FIGURE 2 Amplitude dispersion curves for modulation cycles with unequal "on" and "off" relaxation times. Curves were calculated from Eq. 6. For curve at extreme left of plot $\tau_1 = \tau_{-1} = 10$ s. For remaining curves $\tau_1 = 1$ s and proceeding from left to right, $\tau_{-1} = 10$, 2, and 1 s, respectively. Frequency is in units of πs^{-1}.

The time course of the response (Eqs. 4 and 5) may be represented in terms of the amplitude response function (Eq. 6). For this representation a steady-state cycle is considered, and the time scale is arbitrarily set to extend from 0 to $2\pi/\omega$. The response function is defined so that its amplitude varies from 0 to ΔA as shown in Fig. 1. This function is given by:

$$A(t) = \Delta A \frac{(1 - e^{-t/\tau_1})}{(1 - e^{-\pi/\tau_1})}$$

$$0 < t < \pi/\omega$$

$$A(t) = A\, e^{\pi/\omega\tau_{-1}} \frac{(e^{-t/\tau_{-1}} - e^{-2\pi/\omega\tau_{-1}})}{(1 - e^{-\pi/\omega\tau_{-1}})}.$$

$$\pi/\omega < t < 2\pi/\omega. \tag{8}$$

These equations are similar to those derived previously by a different method (see Eq. a11 of reference 6). In the limit of $k_1 \ll k_{-1}$ the equations are identical once the constant of integration is introduced in the previous work. In the next section a Fourier decomposition is performed on the function in Eq. 8. This allows the identification of the Fourier components, which are detected by a lock-in amplifier.

FOURIER DECOMPOSITION AND HARMONIC SENSITIVITY OF THE DETECTOR

In most modulation experiments the response of the system is measured using a phase-sensitive detector. Amplitudes measured in such experiments will not be those given by Eq. 6. This is because the detector will not equally amplify

all the harmonics of the system's response. It is therefore important to know the harmonic sensitivity of the amplifier to determine the mathematical form of the measured quantity. The harmonic sensitivity of commercial amplifiers commonly falls into one of two different categories. The "tuned" amplifier will solely respond to the principal harmonic of the input signal. All other harmonics are not detected. The "flat" amplifier responds to all the odd harmonics of the input. However, it does not amplify each harmonic evenly. The contributions of each of the odd harmonics to the measured amplitude is proportional to $1/n$, where n is the order of the harmonic. To derive expressions for the measured amplitudes, the system response, Eq. 8, is expressed in terms of its Fourier components. This is done by performing a Fourier decomposition on the response function, $A(t)$. This function is represented as the following Fourier series:

$$A(t) = \sum_{n=-\infty}^{\infty} c_n e^{jn\omega t} \tag{9}$$

where

$$c_n = (\omega/2\pi) \int_0^{2\pi/\omega} A(t) e^{-jn\omega t}\, dt.$$

In the above expressions j equals the square root of -1. The Fourier integral is divided into two parts. The amplitude response function for the "on cycle" (Eq. 8) is integrated from 0 to π/ω, and the function for the "off cycle" (Eq. 8) is integrated from π/ω to $2\pi/\omega$. In the case of low actinic light intensity, $\tau_1 = \tau_{-1}$, the Fourier coefficients are given by:

$$\begin{aligned} c_n(\text{even } n) &= 0 \\ c_0 &= [A]_o \\ c_n(\text{odd } n) &= [A]_o[n\pi(j - n\omega\tau)]^{-1}. \end{aligned} \tag{10}$$

Eq. 10 shows that only the odd harmonics will contribute to the modulated signal. By substituting Eq. 10 into Eq. 9 and combining positive and negative exponentials of the same harmonic, the following expression is obtained:

$$A(t) = \sum_{n=0} \frac{[A]_o \sin[\pi(2n+1)t - \phi_n]}{(2n+1)[1 + \omega^2\tau^2(2n+1)^2]^{1/2}}. \tag{11}$$

The phase shift for each harmonic is given by $\tan \phi_n = (n+1)\omega\tau$. The "tuned" amplifer locks-in on the principal harmonic and measures its amplitude. Thus, in this case the familiar amplitude response function, A_{exp}, is the measured quantity

$$A_{exp} = [A]_o(1 + \omega^2\tau^2)^{-1/2}. \tag{12}$$

This is the same response function that is obtained for a linear response to a sinusoidal perturbation (10). For some amplifiers at low actinic light intensities, it is then appropriate to treat the square wave actinic light as a sinusoidal perturbation. The "flat" amplifier locks-in on the principal harmonic and phase shifts all the odd harmonics so that they are amplified by $1/n$. "Locking-in" on the principal harmonic means that its amplitude will be fully measured. This is equivalent to $\omega t = \phi_0 + \pi/2$. The experimentally measured amplitude is then given by:

$$A_{exp} = \sum_{n=0} \frac{[A]_o \sin[(2n+1)(\pi/2 + \phi_0) - \phi_n]}{(2n+1)^2[1 + \omega^2\tau^2(2n+1)^2]^{1/2}}. \tag{13}$$

This response function can be evaluated extremely precisely by using Eq. 13 and truncating the series at $n = 50$. A truncated series can be used without difficulty in most nonlinear least squares fitting procedures. Therefore, the form of this expression offers no difficulty for data analyses. For comparison Fig. 3 shows the actual response of the system (Eq. 6), the response of the "tuned" amplifier (Eq. 12), and the response of the "flat" amplifier (Eq. 13) for a given set of conditions. As can be seen from this figure, the harmonic sensitivity of the amplifier can have a large effect on the frequency dependence of the measured amplitude.

In the more general case in which τ_1 does not equal τ_{-1}, the Fourier components of the signal are more complicated. In this situation the even harmonics now make a contribution to the signal. However, because most lock-in amplifiers do not detect even harmonics, they can be ignored. The Fourier coefficients for the odd harmonics are given by:

$$\begin{aligned} c_n = \frac{K\omega}{2\pi}\left(\frac{2}{jn} - \frac{1 + e^{-\pi/\omega\tau_1}}{1/\tau_1 + jn\omega}\right) \\ + \frac{K'\omega}{2\pi}\left[\frac{-(1 + e^{-\pi/\omega\tau_{-1}})}{1/\tau_{-1} + jn\omega} + \frac{2\,e^{-\pi/\omega\tau_{-1}}}{jn\omega}\right], \end{aligned} \tag{14}$$

where $K = A/(1 - e^{-\pi/\omega\tau_1})$ and $K' = \Delta A/(1 - e^{-\pi\omega\tau_{-1}})$. Using Eq. 14 in the Fourier series and combining terms as before gives the following representation of $A(t)$:

$$\begin{aligned} A(t) = \sum_{\substack{n=1 \\ \text{odd } n}} \frac{K \sin(n\omega t - \phi_{1,n})}{2\pi(1 + n^2\omega^2\tau_1^2)^{1/2}} \\ + \frac{K'e^{-\pi/\omega\tau_{-1}} \sin(n\omega t - \phi_{-1,n})}{2\pi(1 + n^2\omega^2\tau_{-1}^2)^{1/2}} - \frac{A\omega\tau_1 \sin(n\omega t - \phi_{1,n})}{2\pi[1 + n^2\omega^2\tau_1^2]^{1/2}} \\ + \frac{A\omega\tau_{-1} \sin(n\omega t - \phi_{-1,n})}{2\pi(1 + n^2\omega^2\tau_{-1}^2]^{1/2}}. \end{aligned} \tag{15}$$

Eq. 15 may be used to derive expressions for the measured amplitudes in a similar manner as in the previous case. The resulting form for the measured amplitude will present difficulties for data analyses. This is not because of the complexity of the function but rather because an additional variable must be fit. Unless highly accurate amplitude data can be obtained, it is advantageous to perform the experiment in the regime where the simpler expressions will apply. The condition in which the simple expressions

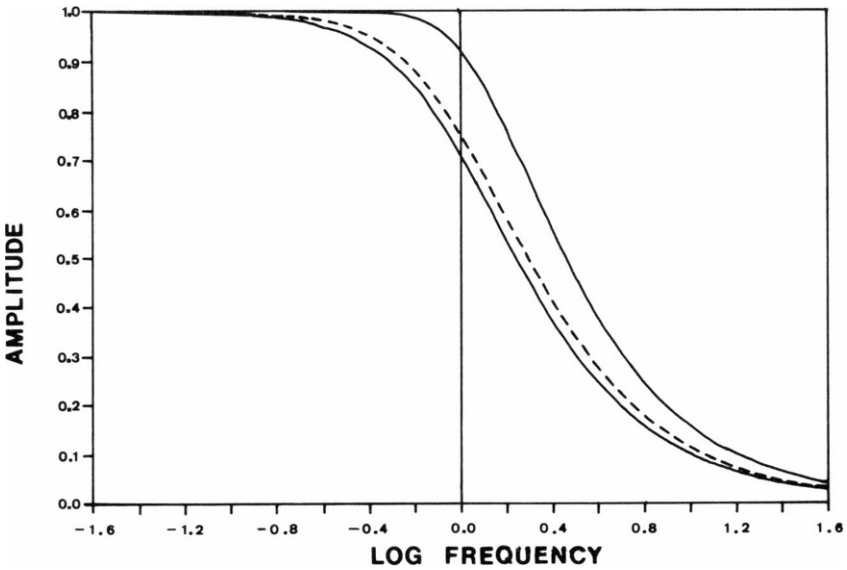

FIGURE 3 Amplitude dispersion curves demonstrating the effect of the harmonic sensitivity of the amplifier. Curve at the extreme left (*solid line*) is calculated for the "tuned" amplifier using Eq. 12 in the text. Middle curve (*dashed line*) is calculated for the "flat" amplifier using Eq. 13. Curve at the extreme right (*solid line*) is calculated for the system response using Eq. 6. All relaxation times are 1.0 s and frequency is in units of πs^{-1}.

are applicable is when $k_1 \ll k_{-1}$. At steady state $k_1 [A]_{ss} = k_{-1}[B]_{ss}$, where the concentrations are at steady-state levels and the chopped actinic light represents small deviations from these concentrations. By experimentally measuring the ratio $[B]_{ss}/[A]_{ss}$, it is possible to assess if the conditions exist for applying the simpler amplitude analysis.

THE RELAXATION OF A CHEMIOSMOTIC PROCESS COUPLED TO A MODULATED PHOTOCYCLE

In this section an analysis is presented for the amplitude response of a chemiosmotic relaxation process, which is driven by a light-activated ion transport protein. As before, the light-activated process will be driven by a periodic modulation of the actinic light. This process will result in a chemiosmotic gradient, which can be used to drive a second process. This system could be achieved experimentally by reconstituting bacteriorhodopsin and a second ion transport protein into phospholipid vesicles. If the second protein can be driven by a membrane-potential or a pH gradient then its ion transport process will be coupled to the light-driven process. In such experimental situations the chemical potential of the transported species is perturbed by the driving force and, thereby, alters the equilibrium of the coupled, chemical reaction. This process is illustrated in Fig. 4, which shows the coupled system and examples of the amplitude response for variables of the system. In the following analysis, linear response theory is used to determine the relaxation time, τ, and amplitude of the system. This is done by determining the stationary forced solution to the following first order differential equation (10):

$$\tau(dA/dt) + A = \bar{A}, \tag{16}$$

where A is an observable variable proportional to the concentration of one of the reacting chemical species, and $\bar{A}$ is the periodic forcing function. The solution of Eq. 16 is given by

$$A(t) = \int_0^t \tau^{-1} e^{-(t-\theta)/\tau} \bar{A}(\theta)\, d\theta. \tag{17}$$

In the case of interest the forcing function will be proportional to the photocycle response to the modulation of the actinic light. In the simplest case it is the same form as Eq. 11. Using Eq. 11 for $\bar{A}(\theta)$ and performing the integration

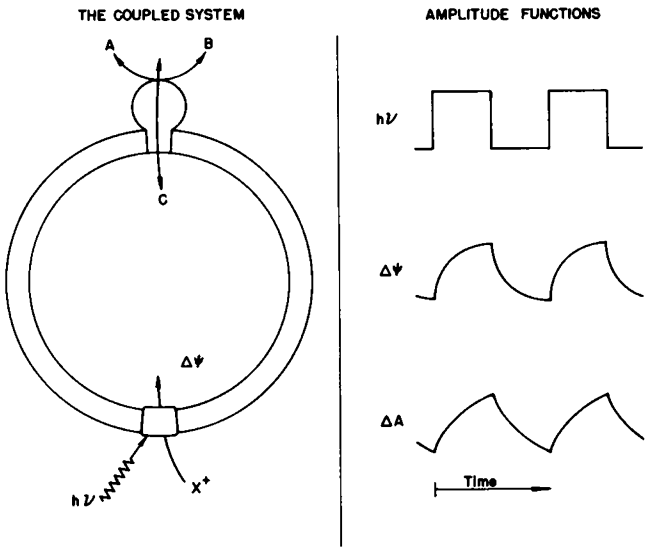

FIGURE 4 Schematic diagram of the chemiosmotic coupling of a light-driven transport process to a chemical transport process. The species X^+ is transported into the interior of the vesicle by a photocycle event and causes the formation of a membrane potential, $\Delta\psi$. The transport of species, C, is driven by the membrane potential and is also coupled to the chemical reaction, $A \rightarrow B$. The time course of several variables of the system is shown on the right-hand side.

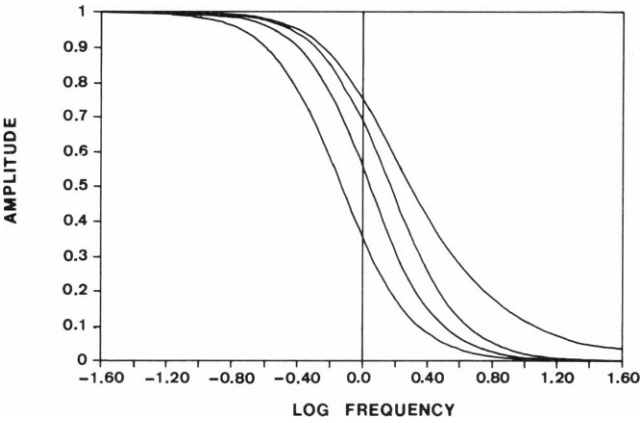

FIGURE 5 Amplitude dispersion curves for a coupled relaxation process. All curves represent detection by the "flat" amplifier. Curve at the extreme right is for the photocycle driving the system with $\tau = 1$ s. This curve was calculated using Eq. 13. Remaining curves represent the response of the coupled system. Moving from left to right, curves have relaxation times of 2, 1, and 0.5 s. All three curves are driven by a photocycle with a $\tau = 1.0$ s and frequency is in units of πs^{-1}.

in Eq. 17 gives

$$A(t) = \sum_{n=0} \cdot \frac{\sin[(2n+1)\omega t - \phi_n - \phi_{D,n}]}{(2n+1)[1+\omega^2\tau^2(2n+1)^2]^{1/2}[1+\omega^2\tau_D^2(2n+1)^2]^{1/2}}, \quad (18)$$

where $\tan \phi_n = (2n+1)\omega\tau$ and $\tan \phi_{D,n} = (2n+1)\omega\tau_D$ define the phase angles for the chemiosmotic process and the photocycle process, respectively. The time constant for the photocycle process, which is driving the reaction, is τ_D. Notice that the integration did not change the order of the harmonics. To determine the amplitude response function, it is again assumed that the maximum amplitude of the principal harmonic is measured. This condition gives: $\omega t - \phi_1 - \phi_{D,1} = \pi/2$. This expression is then substituted into Eq. 18. The harmonic sensitivity of the amplifier can be accounted for in an identical fashion as done previously.

Figs. 5 and 6 show amplitude dispersion curves for different relaxation times of the coupled process. The harmonic sensitivity of the "flat" amplifier was used in generating these curves. As can be seen from the curves in Fig. 5, the dispersion curves are sensitive to changes in the relaxation time of the coupled process. The rate of the light-driven process will limit the time resolution of the technique. However, Fig. 5 shows that it should be possible to measure coupled processes that are twice as fast as the driving process. Fig. 6 shows that for relaxation times that are ten times longer than the forcing time constant, the two processes are almost decoupled. The dispersion curve in this case appears very similar to the one obtained for a light-driven process, which is ten times slower. A reasonably wide range of kinetic behavior should be assessible for this "coupled" experiment. In general, it should be easier to manipulate the relaxation times of the coupled process compared with the photocycle. The concentrations of the reactants in the coupled process could be controlled to provide relaxation times that are slower than that of the photocycle. Current experiments in our laboratory are demonstrating the use of the "coupled" experiment for measuring the relaxation kinetics of the calcium ATPase.

DISCUSSION

A general method is presented for deriving expressions for the amplitude response function observed in phase-lifetime spectroscopic experiments. These functions allow the determination of kinetic parameters for simple photocycles. The method consists of dividing the light-driven modulation experiment into two cycles, the "on" and "off" cycles. The rate expressions for specific mechanisms are

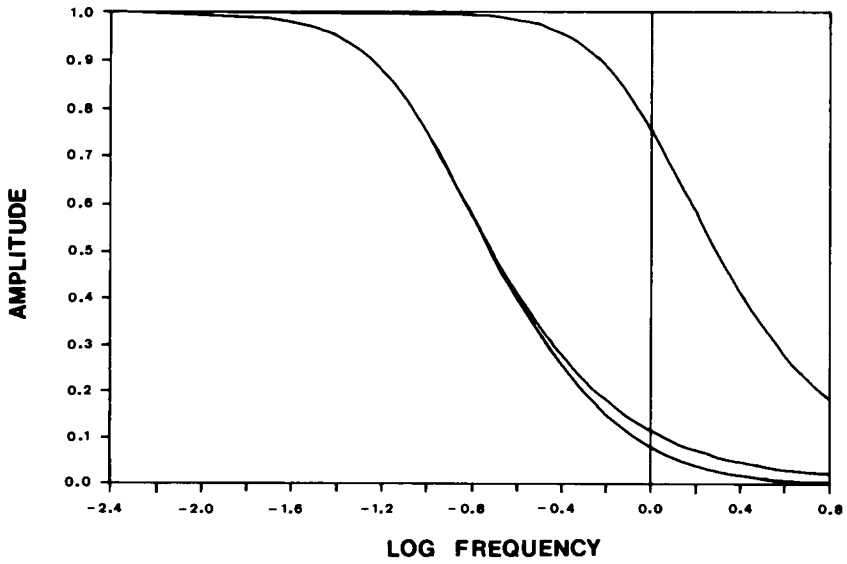

FIGURE 6 Amplitude dispersion curves for photocycle and coupled processes detected with a "flat" amplifier. Curve at extreme left is for a photocycle with a $\tau = 10$ s and is calculated from Eq. 13. The next, nearly identical curve is for a coupled process with $\tau = 10$ s driven by a photocycle with $\tau = 1.0$ s. Curve on the extreme right is for a photocycle with $\tau = 1.0$ s. All frequencies are in units of πs^{-1}.

derived for each cycle. These expressions are "coupled" by the condition that the measured quantity must vary continuously when proceeding from the "on" cycle to the "off" cycle. This condition allows the modulated response of the system to be described in terms of an amplitude and the relaxation times for the exponential growth and decay processes. A Fourier decomposition of this function was performed. This allowed the Fourier components to be weighted by the harmonic sensitivity of the specific lock-in amplifier used. This analysis allows a direct comparison of the kinetic parameters obtained by the modulation experiment with parameters measured by flash techniques. In a future paper (Sinton, M., and T. G. Dewey, manuscript in preparation), this analysis is applied to more complicated photocycle mechanisms. As an extension of this analysis, the case of a second relaxation process coupled to a photocycle process was also considered. Simulated amplitude dispersion curves indicated the range in which the kinetics of the second process could be deconvoluted from the photocycle process. This situation has potential application to the investigation of transmembrane ion-transport kinetics in chemiosmotically coupled systems.

This work was supported by a grant from the National Science Foundation (DMB-8315263).

Received for publication 18 August 1986 and in final form 8 January 1987.

REFERENCES

1. Slifkin, M. A., H. Garty, and S. R. Caplan. 1978. Energetics and Structure of Halophilic Microorganisms. S. R. Caplan and M. Ginzberg, editors. Elsevier, New York. 165–184.
2. Slifkin, M. A., and S. R. Caplan. 1975. Modulation excitation spectrophotometry of purple membrane of *Halobacterium halobium*. *Nature (Lond.)*. 253:56–58.
3. Slifkin, M. A., and M. I. Darby. 1978. Kinetic analysis with a modulation excitation spectrophotometer. *J. Phys. E. Sci. Instrum.* 11:1166–1168.
4. Dewey, T. G., and G. G. Hammes. 1981. Method for studying light-induced transport across membranes. *Proc. Natl. Acad. Sci. USA.* 78:7422–7425.
5. Krupinsky, J., J. L. Spudich, and G. G. Hammes. 1983. Phase-lifetime spectrophotometry of membranes from ion flux mutants of *Halobacterium halobium*. *J. Biol. Chem.* 258:7964–7967.
6. Hasselbacher, C. A., D. K. Preuss, and T. G. Dewey. 1986. Location of the retinal of bacteriorhodopsin's M_{412} intermediates by phase modulation of resonance energy transfer. *Biochemistry.* 25:668–676.
7. Krupinsky, J., and G. G. Hammes. 1985. Phase-lifetime spectrophotometry of deoxycholate purified bacteriorhodopsin reconstituted into asolectin vesicles. *Biochemistry.* 24:6963–6972.
8. Slifkin, M. A., and R. H. Walmsley. 1970. A simple apparatus for measuring the absorption spectrum and lifetimes of photoproduced short lived species using commercial subunits. *J. Phys. E Sci. Instrum.* 3:160–162.
9. Eigen, M., and L. deMaeyer. 1974. Theoretical basis of relaxation methods. *In* Techniques of Chemistry. Vol. 6. G. G. Hammes, editor. Wiley Interscience, New York. 63–146.
10. Prigogine, I. 1955. Introduction to Thermodynamics of Irreversible Processes. Charles C. Thomas, Publisher, Springfield, IL. 47–55.